GTPase activity of dynamin and resulting conformation change are essential for endocytosis

Bruno Marks*†, Michael H. B. Stowell*†, Yvonne Vallis*†, Ian G. Mills*, Adele Gibson‡, Colin R. Hopkins‡ & Harvey T. McMahon*

** MRC Laboratory of Molecular Biology, Hills Road, Cambridge CB2 2QH, UK*
‡ MRC Laboratory for Molecular Cell Biology, University College London, Gower Street, London WC1E 6BT, UK
† These authors contributed equally to this work

Dynamin is a large GTPase with a relative molecular mass of 96,000 (M_r 96K) that is involved in clathrin-mediated endocytosis and other vesicular trafficking processes[1,2]. Although its function is apparently essential for scission of newly formed vesicles from the plasma membrane, the nature of dynamin's role in the scission process is still unclear[3,4]. It has been proposed that dynamin is a regulator (similar to classical G proteins) of downstream effectors[5]. Here we report the analysis of several point mutants of dynamin's GTPase effector (GED) and GTPase domains. We show that oligomerization and GTP binding alone, by dynamin, are not sufficient for endocytosis *in vivo*. Rather, efficient GTP hydrolysis and an associated conformational change are also required. These data argue that dynamin has a mechanochemical function in vesicle scission.

Temperature-sensitive mutants of the *Drosophila* homologue of dynamin, *shibire*, have a paralytic phenotype at the non-permissive temperature due to a reversible blockade of synaptic vesicle recycling[6,7]. An accumulation of deeply invaginated membrane profiles, apparently of vesicles unable to detach from the plasma membrane, is observed in the paralysed flies[8]. On the basis of the *shibire* phenotype it was proposed that dynamin is involved in scission of nascent endocytic vesicles from the plasma membrane. This hypothesis has been strengthened by overexpression studies using dynamin mutants[9–11], and by the observation of a *shibire*-like blockade of endocytosis in GTP-γS-treated synaptosomes[12].

In vitro, dynamin tubulates acidic phospholipid vesicles by helical oligomerization[13,14]. Notably, the GTPase activity of dynamin is increased up to 1,000-fold by its adoption of such a helical conformation[15]. On these lipid nanotubes, GTP hydrolysis by dynamin results in a change in its conformation that can be observed as a dramatic increase in helical pitch (from 11 ± 2 to 20 ± 3 nm)[15]. Some studies have also reported fission of lipid tubules by dynamin (possibly involving a pinching/constriction action)[13,16]. These observations and others suggest that dynamin is a mechanochemical enzyme that uses energy from GTP hydrolysis to generate the force required for membrane scission. However, recent work on GTPase-effector-domain (GED, see Fig. 1) mutants has cast doubt on this hypothesis by demonstrating that dynamin's GTPase activity (stimulated by oligomerization) is not required for endocytosis[5]. This has led to the alternative hypothesis that dynamin is a regulator of downstream effectors of scission, rather than being directly responsible for it. In an effort to distinguish between these two hypotheses, we designed mutants of dynamin that would enable us to test the relationship between dynamin's GTPase activity and its ability to support endocytosis.

Previous studies have implicated the GED of dynamin (Fig. 1) as the physiological activator of dynamin's GTPase activity[5,17]. On the basis of the assumption that the dynamin GED is a GTPase-activating protein (GAP), we mutated all arginine and lysine residues in the GED. Mutants were tested using an *in vivo* assay for endocytosis (see Methods). Within the sensitivity range of our assay, none of the GED mutants seemed to have a significant inhibitory effect on endocytosis of transferrin (Fig. 2; and data not shown). We chose to examine the R725A and K694A mutants of the GED further, as these are the GED mutants known to inhibit dynamin's GTPase activity (stimulated by oligomerization)[5]. We found that the GTPase activity of these mutants was comparable to that of wild-type dynamin (Fig. 2 and Table 1). In our GTPase assay we used lipid nanotubes as the template for oligomerization-dependent stimulation of dynamin's GTPase activity. Previously, the activity of K694A and R725A were assayed using microtubules as the template for oligomerization[5]. We have also assayed these mutants on microtubules and show that K_{cat} (catalytic constant) values for wild type, K694A and R725A are not significantly different (see Supplementary Information). We therefore conclude that dynamin's GED is probably not a GAP in the classical sense (that is, contributing a catalytic residue to the active site). More data and further discussion of these mutants can be found in the Supplementary Information. Notably, several well characterized motor proteins, such as kinesin and myosin, do not use an arginine finger in their catalytic mechanism. The structure of a large dynamin-like GTPase GTP-binding protein has been determined[18], which showed that the phosphate-binding site was completely shielded from solvent, such that a potential GTPase-activating protein cannot approach. Thus, it is not unexpected that we cannot identify a catalytic arginine or lysine residue in dynamin's GED.

What is the possible function of dynamin's GED? In limited proteolysis experiments, the GED of dynamin co-purifies with the GTPase domain, and is probably involved in dynamin oligomerization[5,17]. Deletion analysis of the GED has strengthened this hypothesis[19]. Furthermore, mutations in the GED reverse the reticular phenotype (oligomerized state) of a mutant (T65A; see below) (Fig. 2), supporting the proposed function of this domain in oligomerization.

Guided by the structure of Ras GTPase[20], we made several point mutations in and around the GTP-binding motifs (Fig. 1),

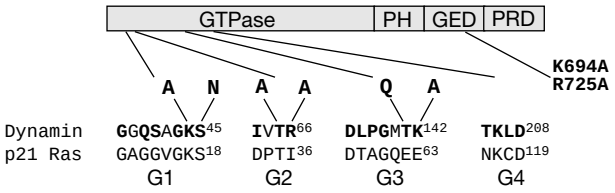

Figure 1 Domain structure of dynamin showing mutants of the GTPase domain. The nucleotide-binding sequences (G1–G4) of dynamin and p21 Ras are compared. Point mutations that we made are shown above the dynamin sequence. The bold residues in dynamin are conserved in dynamin family proteins from *Arabidopsis* to mammals. In addition to a GTPase domain, dynamins possess three other distinct and conserved domains. The pleckstrin homology (PH) domain binds to PtdIns(4,5)P_2-containing lipids[24,25]. The GTPase effector domain (GED) is proposed to be involved in dynamin oligomerization and also activation of dynamin's GTPase activity[5,17,19,26]. The proline/arginine-rich domain (PRD) at the carboxy terminus binds to many SH3-domain-containing proteins including amphiphysin and endophilin[27–29].

Table 1 Kinetic parameters K_{cat} and K_m for a number of dynamin mutants

Dynamin identity	Turnover rate (K_{cat}) (s)	K_m (μM)
Wild type	3.1 ± 0.5	7.8 ± 2.5
S45N	0.083 ± 0.043	ND
T65A	0.023 ± 0.015	9.1 ± 1.1
R66A	0.45 ± 0.19	65.0 ± 5.3
T141Q	0.55 ± 0.15	7.6 ± 3
K142A	1.8 ± 0.4	6.7 ± 1.5
K694A	2.7 ± 0.5	ND
R725A	2.8 ± 0.2	4.3 ± 1.8

As the absolute specific activity (K_{cat}) (mean ± s.d.) varied with different preparations of dynamin and lipid nanotubes, the activities of the mutants were calculated as a percentage of wild-type activity determined in the same experiment (see Fig. 2). The absolute activities have been calculated using those percentages and a value for wild-type activity averaged over several different dynamin and lipid nanotube preparations. ND, not determined.

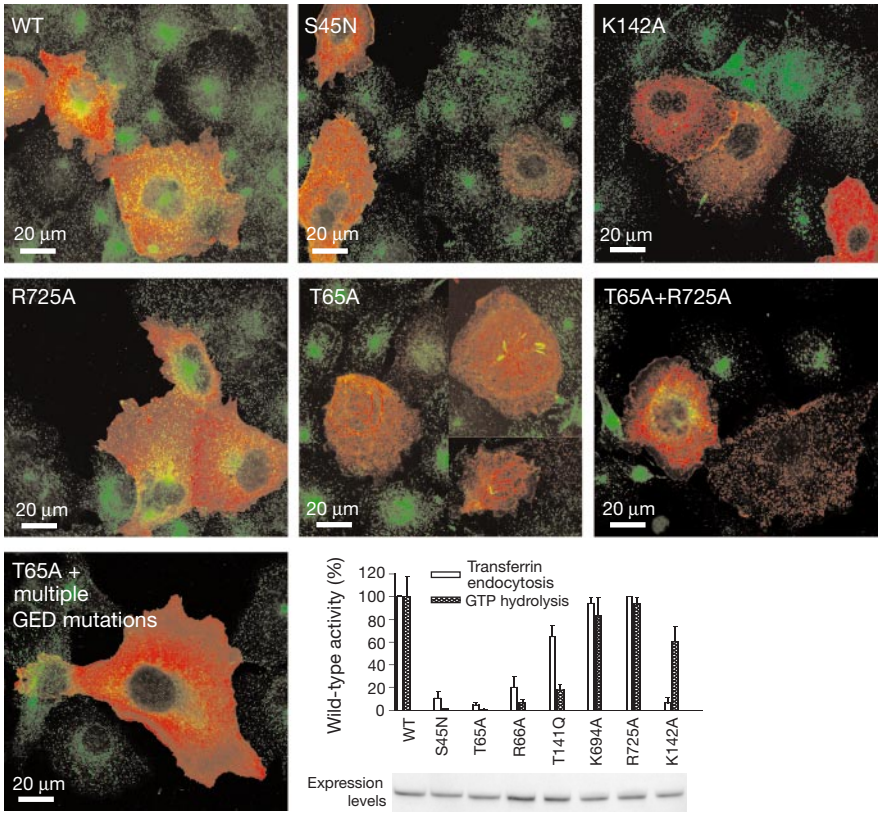

Figure 2 Uptake of biotinylated transferrin (green staining) into COS-7 fibroblasts, transiently overexpressing dynamin or dynamin mutants (red staining). The percentage of transfected cells showing wild-type (WT) transferrin uptake was quantified from several transfection experiments, and is shown in the graph along with a blot showing that there is similar expression of all the dynamin mutants (see Methods). With inhibitory mutants, even weakly expressing cells are strongly inhibited for transferrin uptake (see examples for S45N and K142A). Filled bars show GTP hydrolysis for the purified mutant proteins in the presence of 75 μM GTP. We have presented a number of T65A-expressing cells showing a reticular distribution of dynamin and worms of internalized transferrin. This distribution of T65A dynamin is progressively abolished by mutations of the oligomerization domain. Thus, T65A + R725A show no evidence for worms of transferrin and a reduced tubular appearance. T65A + F698A + R724E + R725E (multiple GED mutations) shows a predominantly cytoplasmic distribution of dynamin similar to WT dynamin transfections. This mutant also shows some uptake of transferrin at a perinuclear localization.

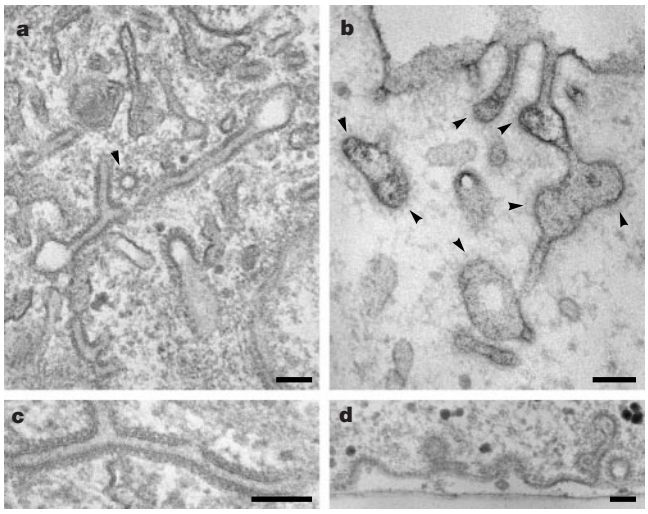

Figure 3 Thin-section electron microscopy of T65A-transfected COS cell. **a**, T65A-transfected cells are full of membrane tubules, many of which emanate from the plasma membrane. Frequently tubules are clearly surrounded by electron density, reminiscent of that seen with dynamin in GTP-γS-treated synaptosomes or on lipid tubules *in vitro*. Cross-sections of these tubules show roughly 10 repeating 'spokes' (see arrowhead). **b**, Plasma-membrane invaginations at the cell surface of cells expressing T65A. Cells were stained with ruthenium red, outlining the continuities with the plasma membrane. Some domains (arrowheads) are clathrin coated. **c**, Tubulated membrane surrounded by electron density that we propose to be dynamin (as no other proteins are being overexpressed in these cells). This correlates with the filamentous dynamin staining seen by immunofluorescence. This represents strong evidence that dynamin can tubulate the plasma membrane *in vivo* as has been shown *in vitro*[14]. **d**, At the plasma membrane of T65A-transfected cells, various intermediate stages of endocytosis were 'captured'. This is reminiscent of what is seen in *shibire Drosophila* at the non-permissive temperature. Scale bar, 0.1 μm.

concentrating on residues that are thought to be directly or indirectly (through coordination of water) involved in catalysis. Initially, mutants were screened using our *in vivo* endocytosis assay. Several inhibitory mutants were identified (Fig. 2). These mutants showed a corresponding inhibition when assayed for GTPase activity, with the exception of K142A (Fig. 2 and Table 1). Further analysis showed that the S45N mutant is defective in GTP binding, as has been predicted[10,11] (see Supplementary Information; and data not shown). Kinetic analysis revealed that R66A has a K_m (Michaelis constant) significantly higher than that of wild-type dynamin (Table 1). The K_m of the other mutants, K142A, T65A and T141Q, are similar to that of wild-type dynamin (Table 1), and are well below the intracellular GTP concentration of 50–150 μM (ref. 21).

If dynamin is a mechanochemical enzyme, GTP hydrolysis must be essential for its function. However, if dynamin acts as a molecular switch in a manner similar to that of classical G proteins, GTP–dynamin would represent the 'on' state, allowing endocytosis to proceed, and GTP hydrolysis would serve to switch it 'off'. A mutant that could bind but not effectively hydrolyse GTP should enable one to distinguish between these two possibilities. The T65A mutant has a very low GTPase activity, but has a K_m close to that of the wild-type dynamin. The fact that this mutant strongly inhibits endocytosis implies that effective GTP hydrolysis by dynamin, and not simply GTP binding, is necessary for vesicle scission.

Of note, in our *in vivo* endocytosis assay, roughly 50% of cells expressing T65A had a very distinctive appearance (seen also to a lesser extent in T141Q and R66A, see Supplementary Information).

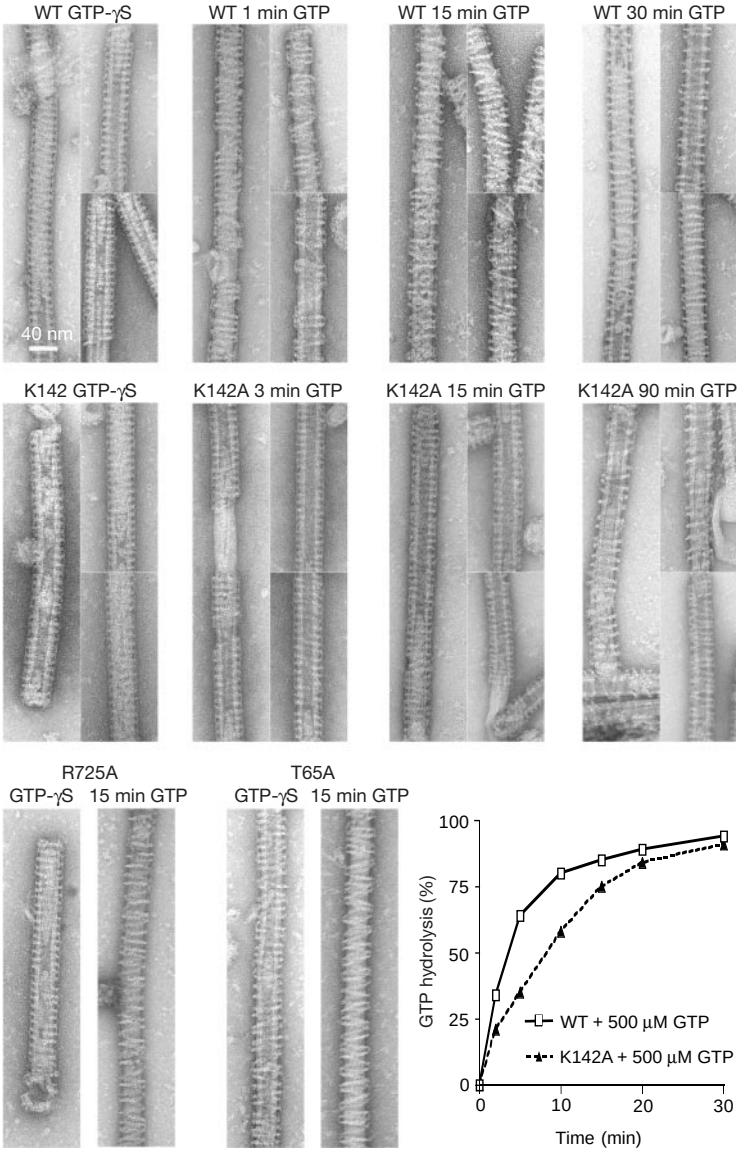

Figure 4 Conformational changes in dynamin on GTP hydrolysis. Purified, expressed dynamin bound to lipid nanotubes were visualized by negative staining in the presence of 100 μM GTP-γS or during the hydrolysis of 500 μM GTP. To compare the extent of GTP hydrolysis at different sampling times for WT versus K142A dynamin, aliquots of the electron microscopy (e-m) reactions were taken for TLC in addition to being put on e-m grids (graph, bottom right). The R725A mutant has essentially the same time-course of GTP hydrolysis as WT dynamin (see Table 1 and Supplementary Information). WT, K142A and R725A dynamin all adopt an ordered, tight, helical conformation in the presence of GTP-γS. In the presence of GTP, much of this order is immediately lost by WT (or R725A) dynamin even at very short time points after hydrolysis. At long time points, WT dynamin is bound in a loose helix about the lipid nanotubes. In contrast, the K142A mutant stays in a conformation similar to that seen with GTP-γS, until most of the GTP has been hydrolysed. T65A dynamin does not adopt a tight, ordered conformation in the presence of GTP-γS, it is looser and disordered. This conformation does not apparently change as a result of GTP hydrolysis. The conformational changes reported here for baculovirus-expressed WT bovine dynamin I are identical to those reported in our previous paper for purified rat brain dynamin, which contains an equal mixture of 96K and 93K spliceforms.

The dynamin in these T65A-expressing cells had the appearance of being localized along thin filaments running throughout the cell (reticular, rather than the predominant cytosolic distribution seen with wild-type protein) (Fig. 2). Although there was no general transferrin staining within T65A-transfected cells (indicating an inhibition of endocytosis) many cells showed discreet, brightly stained 'worms' of transferrin (Fig. 2, T65A panel). Using thin-section electron microscopy, we have shown that the T65A-transfected cells are full of membrane tubules, many of which can be seen to be connected with the plasma membrane (Fig. 3). The tubules are of uniform diameter and are coated with rings of protein that have the same T-bar-like structures as are seen with dynamin bound to lipid nanotubes *in vitro* (compare Fig. 3c to purified dynamin on tubules in Fig. 4). We propose that the T65A dynamin oligomerizes as normal about the necks of invaginating vesicles in its GTP-bound state, but cannot hydrolyse GTP effectively, and therefore does not catalyse the scission reaction. Furthermore, as GTP hydrolysis is so impaired, the T65A dynamin has a much longer lifetime on the plasma membrane than would wild-type dynamin, and is therefore able to form long oligomers that create tubular membrane invaginations. We believe that the worms of transferrin that are sometimes observed in T65A-expressing cells are transferrin that has undergone endocytosis at the end of these tubular invaginations. Some of these invaginations may fuse (as endocytic vesicles would to form early endosomes) resulting in a transferrin-rich compartment that is still contiguous with the extracellular environment. We have used ruthenium red staining to confirm the surface accessibility of much of the tubulated membrane (Fig. 3). Using immuno-gold labelling, we observed that transferrin is often concentrated at the intracellular ends of the tubules (data not shown).

The T65A mutant supports the hypothesis that further to formation of a dynamin–GTP oligomer around a vesicle neck, GTP hydrolysis is necessary for scission to occur. Another mutant that we identified, T141Q, further supports this hypothesis. T141Q is partially inhibited in its GTPase activity and correspondingly it partially inhibits endocytosis (Fig. 2 and Table 1). Owing to the limitations of our endocytosis assay and the conservative criteria by which inhibition is 'scored', the extent of partial inhibition by T141Q is probably underestimated (see Methods). Nevertheless, for these mutants, there is a direct correlation between the degree of endocytic inhibition and inhibition of their GTPase activity, an expected result if GTP hydrolysis is directly required in the process of vesicle scission.

In contrast, the K142A mutant has only a moderately impaired GTPase activity (Table 1), but inhibits endocytosis strongly (Fig. 2). Initially, this finding seems to be incompatible with currently proposed hypotheses for dynamin's action. Because of this apparent anomaly, we chose K142A for further investigation. Previously we have shown that wild-type dynamin, oligomerized into a helix about PIP_2-containing lipid nanotubes, extends its pitch on GTP hydrolysis[15]. Figure 4 shows that with wild-type dynamin, a conformational change resulting in an average increase in helical pitch from 11 ± 2 nm to 15 ± 2 nm (mean $\pm$ s.d.) is evident at the shortest GTPase assaying times that we tested (after 1 min, which equates to about 25% GTP hydrolysis). With K142A, after equivalent GTP hydrolysis (3 min or 25% hydrolysis), the pitch of the dynamin helix had not changed significantly from that observed with K142A-GTP-γS (11 ± 2 nm and 11 ± 1 nm, respectively). In fact, K142A dynamin did not change conformation from a tightly wound helical state until all of the GTP had been hydrolysed (which will never occur *in vivo*). This suggests that the catalytic cycle of K142A is defective in such a way that if there is any GTP available to bind, this occurs without the previous transition through a loosely helical GDP state. At present we do not have a precise understanding of the mechanistic defect present in K142A, but these observations suggests that as well as efficient GTP hydrolysis, a conformational change in dynamin is required for endocytosis, that is, mechanochemical coupling. The conformational change could be coupled to one of several steps in the catalytic cycle, such as hydrolysis, product release and/or a subsequent isomerization step.

We also examined the conformations of other dynamin mutants bound to lipid nanotubes. R725A behaved exactly as wild-type dynamin (Fig. 4). K694A, although not examined as thoroughly, also showed wild-type characteristics (data not shown). The T65A mutant did not form a tight, ordered conformation with GTP-γS (average pitch 12 ± 2 nm). Its inability to hydrolyse GTP rapidly could be related to this.

It is interesting to note that after extensive GTP hydrolysis by wild-type dynamin we observe an increase in the percentage of dynamin showing increased helical pitch; however, we rarely observe the uniformity of conformation seen when dynamin is incubated with GDP[15]. This may be because GTP is never completely depleted in our experiments.

We have demonstrated a positive correlation between the GTPase activity of dynamin and its ability to support endocytosis *in vivo*. In addition, an anomaly to this correlation, K142A, was found to be defective in its ability to change conformation while still maintaining high GTPase activity. Thus, dynamin's function in endocytosis requires both GTP hydrolysis and a resulting conformational change before, or concomitant with, vesicle scission. □

Methods

Transferrin uptake

We transfected COS-7 fibroblasts using DEAE dextran. Thirty-six hours after transfection, cells were transferred to serum-free medium and incubated overnight. The next day, the cells were incubated for 30 min at 37 °C in the presence of 25 ug ml^{-1} biotinylated human transferrin (Sigma), and then fixed (4% paraformaldehyde). Transferrin uptake was visualized using FITC-conjugated streptavidin (green) on an MRC 1024 scanning confocal microscope. We detected dynamin using an anti-dynamin polyclonal antibody (Ra19), followed by Texas Red-conjugated anti-rabbit antibody (Chemicon). Inhibition of endocytosis in transfected cells was defined as transferrin uptake less than 20% of that seen in untransfected cells in the same field. This ensures that only strongly inhibited cells are scored. A consequence of this is that the degree of inhibition of partially inhibitory mutants might be underestimated (for example, T141Q). In all mutants that were inhibited in transferrin uptake, dynamin no longer had a predominantly cytoplasmic distribution. With cells expressing T65A mutant dynamin, a filamentous appearance could be observed. The density and length of filaments was expression-level dependent. In Fig. 2, T65A is a serial reconstruction, rather than a single confocal section, to better illustrate these observations.

Dynamin expression and purification

Wild-type dynamin (bovine dynamin 1) and mutants were expressed using the baculovirus pBac 4 system (Novagen) and purified using a recombinant, bacterially expressed, GST-tagged, amphiphysin-2 SH3 domain as an affinity ligand, as described[15]. The quality of dynamin was regularly checked by SDS-PAGE and Coomassie staining, and dynamin was not used if more than roughly 5% degraded.

GTPase assays

GTPase assays were carried out both as described, using thin-layer chromatography (TLC)[15], and by a continuous enzyme-coupled method for monitoring phosphate release (EnzChek, Molecular Probes). With both methods reactions were as follows. Reaction volumes were 20 μl for the TLC assay and 60 μl for the enzyme-coupled assay. Lipid nanotubes (0.1 mM lipid) and dynamin (typically 0.5 μM) were incubated for 10 min at room temperature in buffer A (135 mM NaCl, 5 mM KCl, 20 mM HEPES, 1 mM MgCl2) and then reactions were initiated by the addition of GTP (5–500 μM). For the continuous enzyme-coupled assay, purine nucleotide phosphorylase (20 U ml^{-1}) and 2-amino-6-mercapto-7-methylpurine ribonucleoside (MESG) (200 μM) were also present in the reaction mix from the beginning. After initiation of the reaction its progress was monitored as an increase in A_{355} (due to the phosphate-dependent conversion of MESG to ribose-1-phosphate and 2-amino-6-mercapto-7-methylpurine) using a Hewlett Packard spectrophotometer. For the TLC assay, the GTP was spiked with about 10 μCi ml^{-1} [α^{32}P] GTP. The extent of GTP hydrolysis at distinct time points during the course of a reaction was analysed by TLC on PEI cellulose (Sigma), and results were quantified using a phosphoimager and ImageQuant software (Molecular Dynamics). We transferred raw data to the GraphPad suite of kinetic analysis programs for determination of the kinetic parameters K_{cat} and K_m.

Preparation of lipid nanotubes

We prepared lipid nanotubes essentially as described[15,22]. The lipid composition (w/w) was 40% phosphatidylcholine, 40% non-hydroxy fatty acid galactocerebroside, 10% cholesterol and 10% phosphoinositide 4,5-bisphosphate (PtdIns(4,5)P_2). The nanotubes

produced had an average diameter of 28 nm (with little variation) and an average length of 500 nm.

Electron microscopy of dynamin on lipid nanotubes

Samples for electron microscopy were prepared as for GTPase assay reactions in the presence of 100 μM GTP-γS or 500 μM GTP. Samples were applied to glow-discharged 350-mesh grids that were carbon-coated, stained with 0.5% uranyl acetate, and imaged on a Philips 208 80-kV electron microscope.

Thin section electron microscopy of COS-7 cells

COS-7 cells were transfected with T65A dynamin as for transferrin-uptake assays. Cells were fixed with 2% paraformaldehyde/1.5% glutaraldehyde in 0.1 M sodium cacodylate for 20 min at room temperature. Cells were post-fixed in 1% osmium tetroxide/1.5% potassium ferricyanide and then treated with tannic acid. We then embedded cells as described[23]. To test for surface accessibility of tubules, cells were fixed with 2% paraformaldehyde/1.5% gluteraldehyde/0.3% ruthenium red, for 30 min at room temperature. These cells were post-fixed in 1% osmium tetroxide/0.3% ruthenium red, for 1 h at 4 °C, followed by dehydration and embedding. Thin sections were cut on a Reichert-Jung Ultracut E ultramicrotome, stained with lead citrate and viewed using a Phillips CM12 transmission electron microscope.

Received 29 September; accepted 18 January 2001.

1. Urrutia, R., Henley, J. R., Cook, T. & McNiven, M. A. The dynamins: redundant or distinct functions for an expanding family of related GTPases? *Proc. Natl Acad. Sci. USA* **94,** 377–384 (1997).
2. van der Bliek, A. M. Functional diversity in the dynamin family. *Trends Cell Biol.* **9,** 96–102 (1999).
3. Warnock, D. E., HInshaw, J. E. & Schmid, S. L. Dynamin self-assembly stimulates its GTPase activity. *J. Biol. Chem.* **271,** 22310–22314 (1996).
4. Roos, J. & Kelly, R. B. Is dynamin really a 'pinchase'? *Trends Cell Biol.* **7,** 257–259 (1997).
5. Sever, S., Muhlberg, A. B. & Schmid, S. L. Impairment of dynamin's GAP domain stimulates receptor-mediated endocytosis. *Nature* **398,** 481–486 (1999).
6. Poodry, C. A. & Edgar, L. Reversible alterations in the neuromuscular junctions of *Drosophila melanogaster* bearing a temperature-sensitive mutation, shibire. *J. Cell Biol.* **81,** 520–527 (1979).
7. Kosaka, T. & Ikeda, K. Possible temperature-dependent blockage of synaptic vesicle recycling induced by a single gene mutation in *Drosophila*. *J. Neurobiol.* **14,** 207–225 (1983).
8. Koenig, J. H. & Ikeda, K. Disappearance and reformation of synaptic vesicle membrane upon transmitter release observed under reversible blockage of membrane retrieval. *J. Neurosci.* **9,** 3844–3860 (1989).
9. van der Bliek, A. M. *et al.* Mutations in human dynamin block an intermediate stage in coated vesicle formation. *J. Cell Biol.* **122,** 553–563 (1993).
10. Herskovits, J. S., Burgess, C. C., Obar, R. A. & Vallee, R. B. Effects of mutant rat dynamin on endocytosis. *J. Cell Biol.* **122,** 565–578 (1993).
11. Damke, H., Baba, T., Warnock, D. E. & Schmid, S. L. Induction of mutant dynamin specifically blocks endocytic coated vesicle formation. *J. Cell Biol.* **127,** 915–934 (1994).
12. Takei, K., McPherson, P. S., Schmid, S. L. & DeCamilli, P. Tubular membrane invaginations coated by dynamin rings are induced by GTPγS in nerve terminals. *Nature* **374,** 186–190 (1995).
13. Sweitzer, S. M. & Hinshaw, J. E. Dynamin undergoes a GTP-dependent conformational change causing vesiculation. *Cell* **93,** 1021–1029 (1998).
14. Takei, K. *et al.* Generation of coated intermediates of clathrin-mediated endocytosis on protein-free liposomes. *Cell* **94,** 131–141 (1998).
15. Stowell, M. H. B., Marks, B., Wigge, P. & McMahon, H. T. Nucleotide-dependent conformational changes in dynamin: evidence for a mechanochemical molecular spring. *Nature Cell Biology* **1,** 27–32 (1999).
16. Takei, K., Slepnev, V. I., Haucke, V. & De Camilli, P. Functional partnership between amphiphysin and dynamin in clathrin-mediated endocytosis. *Nature Cell Bio.* **1,** 33–39 (1999).
17. Muhlberg, A. B., Warnock, D. E. & Schmid, S. L. Domain structure and intramolecular regulation of dynamin GTPase. *EMBO J.* **16,** 6676–6683 (1998).
18. Prakash, B., Renault, L., Praefcke, G. J., Herrmann, C. & Wittinghofer, A. Triphosphate structure of guanylate-binding protein 1 and implications for nucleotide binding and GTPase mechanism. *EMBO J.* **19,** 4555–4564 (2000).
19. Okamoto, P. M., Tripet, B., Litowski, J., Hodges, R. S. & Vallee, R. B. Multiple distinct coiled-coils are involved in dynamin self-assembly. *J. Biol. Chem.* **274,** 10277–10286 (1999).
20. Pai, E. F. *et al.* Refined crystal structure of the triphosphate conformation of H-ras p21 at 1.35 A resolution: implications for the mechanism of GTP hydrolysis. *EMBO J.* **9,** 2351–2359 (1990).
21. Otero, A. D. Transphosphorylation and G protein activation. *Biochem. Pharmacol.* **39,** 1399–1404 (1990).
22. Wilson-Kubalek, E. M., Brown, R. E., Celia, H. & Milligan, R. A. Lipid nanotubes as substrates for helical crystallization of macromolecules. *Proc. Natl Acad. Sci. USA* **95,** 8040–8050 (1998).
23. Hopkins, C. R. & Trowbridge, I. S. Internalization and processing of transferrin and the transferrin receptor in human carcinoma A431 cells. *J. Cell Biol.* **97,** 508–521 (1983).
24. Vallis, Y., Wigge, P., Marks, B., Evans, P. R. & McMahon, H. T. Importance of the pleckstrin homology domain of dynamin in clathrin-mediated endocytosis. *Curr. Biol.* **9,** 257–260 (1999).
25. Achiriloaie, M., Barylko, B. & Albanesi, J. P. Essential role of the dynamin pleckstrin homology domain in receptor mediated endocytosis. *Mol. Cell. Biol.* **19,** 1410–1415 (1999).
26. Smirnova, E., Shurland, D. L., Newman-Smith, E. D., Pishvaee, B. & van der Bliek, A. M. A model for dynamin self-assembly based on binding between three different protein domains. *J. Biol. Chem.* **274,** 14942–14947 (1999).
27. Grabs, D. *et al.* The SH3 domain of amphiphysin binds the proline-rich domain of dynamin at a single site that defines a new SH3 binding consensus sequence. *J. Biol. Chem.* **272,** 13419–13425 (1997).
28. Wigge, P. *et al.* Amphiphysin heterodimers: potential role in clathrin-mediated endocytosis. *Mol. Biol. Cell* **8,** 2003–2015 (1997).
29. Owen, D. J. *et al.* Crystal structure of the Amphiphysin-2 SH3 domain and its role in prevention of dynamin ring formation. *EMBO J.* **17,** 5273–5285 (1998).

Supplementary information is available on *Nature*'s World-Wide Web site (http://www.nature.com) or as paper copy from the London editorial office of *Nature*.

Acknowledgements

We thank P. Wigge for discussions, M. Ford for discussions and assistance with immunofluorescence work, and M. Higgins for help with the expression of dynamin mutants.

Correspondence and requests for materials should be addressed to H.T.M. (e-mail: hmm@mrc-lmmb.cam.ac.uk).

A mechanism for initiating RNA-dependent RNA polymerization

Sarah J. Butcher*†, Jonathan M. Grimes†‡, Eugeny V. Makeyev*, Dennis H. Bamford* & David I. Stuart‡§

** Institute of Biotechnology and Department of Biosciences, Viikki Biocenter, PO Box 56 (Viikinkaari 5), 00014 University of Helsinki, Finland*
‡ Division of Structural Biology, The Henry Wellcome Building for Genomic Medicine, Oxford University, Roosevelt Drive, Oxford OX3 7BN, UK
§ The Oxford Centre for Molecular Sciences, New Chemistry, South Parks Road, Oxford OX1 3QT, UK
† These authors contributed equally to this work

In most RNA viruses, genome replication and transcription are catalysed by a viral RNA-dependent RNA polymerase. Double-stranded RNA viruses perform these operations in a capsid (the polymerase complex), using an enzyme that can read both single- and double-stranded RNA. Structures have been solved for such viral capsids, but they do not resolve the polymerase subunits in any detail[1,2]. Here we show that the 2 Å resolution X-ray structure of the active polymerase subunit from the double-stranded RNA bacteriophage φ6 (refs 3, 4) is highly similar to that of the polymerase of hepatitis C virus, providing an evolutionary link between double-stranded RNA viruses and flaviviruses. By crystal soaking and co-crystallization, we determined a number of other structures, including complexes with oligonucleotide and/or nucleoside triphosphates (NTPs), that suggest a mechanism by which the incoming double-stranded RNA is opened up to feed the template through to the active site, while the substrates enter by another route. The template strand initially overshoots, locking into a specificity pocket, and then, in the presence of cognate NTPs, reverses to form the initiation complex; this process engages two NTPs, one of which acts with the carboxy-terminal domain of the protein to prime the reaction. Our results provide a working model for the initiation of replication and transcription.

φ6 is amenable to reverse genetics and *in vitro* assembly from purified components[5], allowing the dissection of both replication (minus-strand synthesis from single-stranded templates) and semi-conservative transcription (plus-strand synthesis from a double-stranded template)[6,7]. Isolated recombinant φ6 polymerase can use both single-stranded (ss) RNA and double-stranded (ds) RNA as templates with similar elongation rates for the polymerase complex. The rate-limiting step of the transcription reaction is initiation, which occurs at the conserved, terminal 3′-cytidine nucleotide of the negative sense, linear, template RNA[3,8].

We determined the structure of recombinant polymerase by multi-wavelength anomalous dispersion of a single crystal of seleno-methionated protein (see Methods). The twofold-averaged